Available online at www.sciencedirect.com
SCIENCE DIRECT®
Tectonophysics 368 (2003) 71–88
TECTONOPHYSICS
www.elsevier.com/locate/tecto

Comparison of P- and S-wave velocity profiles obtained from surface seismic refraction/reflection and downhole data

Robert A. Williams*,[1], William J. Stephenson, Jack K. Odum

U.S. Geological Survey, Golden, CO, USA

Received 20 August 2002; accepted 10 March 2003

Abstract

High-resolution seismic-reflection/refraction data were acquired on the ground surface at six locations to compare with near-surface seismic-velocity downhole measurements. Measurement sites were in Seattle, WA, the San Francisco Bay Area, CA, and the San Fernando Valley, CA. We quantitatively compared the data in terms of the average shear-wave velocity to 30-m depth (V_{s30}), and by the ratio of the relative site amplification produced by the velocity profiles of each data type over a specified set of quarter-wavelength frequencies. In terms of V_{s30}, similar values were determined from the two methods. There is $<15\%$ difference at four of the six sites. The V_{s30} values at the other two sites differ by 21% and 48%. The relative site amplification factors differ generally by less than 10% for both P- and S-wave velocities. We also found that S-wave reflections and first-arrival phase delays are essential for identifying velocity inversions. The results suggest that seismic reflection/refraction data are a fast, non-invasive, and less expensive alternative to downhole data for determining V_{s30}. In addition, we emphasize that some P- and S-wave reflection travel times can directly indicate the frequencies of potentially damaging earthquake site resonances. A strong correlation between the simple S-wave first-arrival travel time/apparent velocity on the ground surface at 100 m offset from the seismic source and the V_{s30} value for that site is an additional unique feature of the reflection/refraction data that could greatly simplify V_{s30} determinations.

Keywords: Seismic reflection/refraction; S-wave; Site characterization; Site response; Downhole

1. Introduction

According to the Uniform Building Code (Building Seismic Safety Council, 1997), assessing potential earthquake ground motions at a new building site requires classification of the soil profile in the upper 30 m by the U.S. National Earthquake Hazard Reduction Program (NEHRP). The 1997 Uniform Building Code adopted the NEHRP provisions which recommend an assessment of V_{s30} at building sites. The new building code assigns one of six soil profile types, from hard rock (type A) to soft soils (type E or F), to a site, based on the V_{s30} (Table 1). These soil profile categories, which are determined for each of the sites in this study, will also be part of International Building Code to be adopted in 2002 (Building Seismic Safety Council, 2000).

* Corresponding author. U.S. Geological Survey, Denver Federal Center, MS966, Box 25046, Denver, CO 80225, USA. Tel.: +1-303-273-8636; fax: +1-303-273-8600.
E-mail address: rawilliams@usgs.gov (R.A. Williams).
[1] Overnight mail address: U.S. Geological Survey, 1711 Illinois St., Golden, CO 80401, USA.

0040-1951/03/$ - see front matter © 2003 Elsevier Science B.V. All rights reserved.
doi:10.1016/S0040-1951(03)00151-3

Table 1
Site categories in NEHRP provisions (BSSC, 1997)

Soil profile type	Rock/soil description	Average S-wave velocity (m/s) top 30 m
A	Hard rock	>1500
B	Rock	760–1500
C	Very dense soil/ soft rock	360–760
D	Stiff soil	180–360
E	Soft soil	<180
F	Special soils requiring site-specific evaluation	

According to NEHRP guidelines, V_{s30} for a layered structure is determined by:

$$V_{s30} = \frac{\sum_{i=1}^{n} d_i}{\sum_{i=1}^{n} \frac{d_i}{V_{si}}}$$

where d_i is the thickness of the ith layer between 0 and 30 m and V_{si} is the velocity in the ith layer. The soil profile classification can be made using on-site measurements of soil blow counts, unconfined compressive strength, or shear-wave seismic velocity (V_s). Because of their importance and wide use in the engineering community, engineers need alternative ways to measure these three parameters less expensively and less invasively than by traditional borehole methods. Of these three parameters, V_s is the easiest to measure by non-invasive techniques such as surface seismic reflection/refraction, spectral analysis of surface-waves (SASW; Stokoe and Nazarian, 1985), or refraction microtremor (Louie, 2001). Campbell and Duke (1976), King et al. (1990), Williams et al. (1994), and Harris et al. (1994) used these types of surface methods to acquire V_s and V_p (P-wave velocity) data in noisy urban areas where crucial assessment of the earthquake ground-shaking potential is needed. However, despite the growing use of these methods in engineering studies and a time-tested history of success in the oil exploration industry, there remains uncertainty in the earthquake engineering community as to how these measurements of V_s and V_p compare with downhole measurements. Part of this uncertainty probably originates from a tradition of using downhole velocity data in earthquake site response studies. Downhole data also have the added confidence that comes from placement of the sensor physically in the deposits that are being measured. Thus, this study is motivated toward clarifying the differences between surface reflection/refraction data and downhole data by directly comparing independent measurements of near-surface V_s and V_p by these methods.

Use of surface reflection/refraction methods to characterize the near surface is based on two decades of research refining these techniques in field and lab studies. As summarized by Steeples (1998), high quality images of the upper 100 m of ground using reflection/refraction imaging methods have been described in dozens of papers since the early 1980s. For high-resolution P-wave seismic-reflection data acquired with much shorter geophone intervals than used in this study, minimum imaging depths have decreased and resolution limits of thin beds have increased to where layers as shallow as 1 m and beds as thin as 0.1 m can be detected under the right conditions (Steeples, 1998). Because similar seismic sources and sensors are used, minimum imaging depths and resolution limits for seismic-refraction data are comparable to those of seismic-reflection data. Also, in many reflection/refraction studies, the interpreted layer boundaries have been corroborated by the stratigraphy interpreted from borehole data (e.g., Luzietti et al., 1992; Miller et al., 1995; Liberty, 1998). These studies show that reflection/refraction data have become a valuable tool in near-surface studies.

Analysis of reflection/refraction and downhole data in this study shows that, despite significant differences in the subsurface area sampled by these two methods, similar velocity structures are determined. These velocity structures are similar in terms of overall velocity trends determined by visual inspection of velocity–depth profiles, V_{s30} (for NEHRP site categories), and calculated amplification ratios. The main differences in velocity–depth data between the two methods are that the downhole data tend to reveal a slightly greater number of distinct velocity layers over the upper 30 m and a greater number of velocity inversions. The magnitude of these differences suggests that surface reflection/refraction data should not be used instead of downhole data if the study requires a more detailed depiction of velocity structure. This is not to suggest that velocity profiles determined from

the ground surface only are "wrong" because the resolution is not identical to the downhole data, they are merely different mainly because the subsurface areas imaged by the two methods are quite different. Our results suggest that reflection/refraction data would be useful to the earthquake engineer or seismologist who needs a quick assignment of a NEHRP site category or a reliable velocity structure that can be used to help explain earthquake ground motions. We also show that it is unlikely that surface reflection/refraction data will duplicate the downhole velocity log determined by measurements every 1 to 3 m. The decision to use surface methods only must consider these limitations, plus other advantages and disadvantages that are listed below. Some advantages of surface reflection/refraction methods are that it: (1) is less invasive with fewer permitting and environmental complications, (2) is faster (especially when compared to the complete drilling operation, typically, about two sites per day can be acquired), (3) offers a more areally extensive sample of the subsurface, (4) in some cases, can directly detect potentially strong site resonances through reflection travel times (Williams et al., 1998, 1999, 2001), and (5) is less costly by about a factor of 3 to 4: it costs about US$1000 for each reflection/refraction site, including data acquisition and processing, as compared to a 30-m-deep borehole geologically logged by a continuous flight auger and then measured geophysically by downhole methods (J. Tinsley, personal commun., 2001). Some of the disadvantages of using surface reflection/refraction methods versus downhole methods are: (1) velocity inversions can go undetected, (2) there is sometimes a limited depth range due to space and energy source restrictions, (3) no sample of subsurface material is taken and no in-situ testing is possible, (4) data analysis is probably more complicated because it requires analysis and interpretation of reflection and refraction phases rather than just first-arrival travel times, and (5) ambient noise probably has a larger degrading effect on the reflection/refraction data than on downhole data because source signal is more attenuated at the maximum source–receiver offset distances due to the generally greater source–receiver distances used in reflection/refraction methods. We will show that the first disadvantage listed above can sometimes be avoided or have a reduced impact by incorporating reflection data and recognizing velocity inversion indicators in the refracted first-arrival pattern. Disadvantages 2 and 3 are not critical to velocity determinations and also may be outweighed by some of the reflection/refraction advantages. This study is also limited somewhat because, although interpretations of reflection and refraction data should be similar between different interpreters, it uses the results of only one interpreter and one method of interpreting these data.

2. Methodology

2.1. Data acquisition

The six study sites are located in a variety of urban ambient noise conditions in California and Washington (Fig. 1), with a limited range of site geology (Table 2). As described above, noisy conditions from auto traffic, wind, etc., can effect the interpretation of both reflection/refraction and downhole methods, primarily by obscuring the first-arrival phases and introducing errors in picking accurate arrival times. Comparing the amplitudes of pre-first-arrival noise to first-arrival signal we found the signal-to-noise ratios for these reflection/refraction data ranged from about 4 to 8 at HOL, a relatively quiet small rural airport, to about 1 at site PAV, a hospital in an urbanized area (Fig. 2). Surficial geologic deposit types were limited in this study to Quaternary unconsolidated sand, clay, and silt (Table 2).

We selected the six sites listed in Table 2 from among the 60 locations in the western U.S. where we have acquired surface reflection/refraction data. For these six sites, we intentionally positioned the seismic profiles as close as possible to the borehole location so that we could compare the results. The distance between the borehole and the approximate center of the seismic profile and the source reference from which the borehole data were taken are also listed in Table 2.

The reflection/refraction seismic profiles were linear and were located on flat topography in residential areas (paved streets or city parks) or on any open ground as close as possible (inter-site distances ranged from 0 to 175 m) to the borehole. Recording parameters are listed in Table 3. Reversed seismic profiles were 87 m in length, with some unreversed profiles

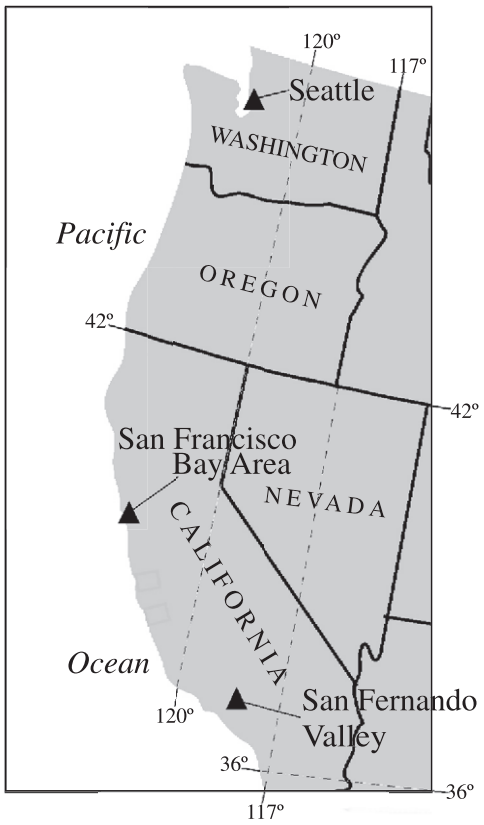

Fig. 1. Map of western United States showing the general location of the three areas (▲), Seattle, Washington, San Francisco Bay Area, California, and San Fernando Valley, California, from which data were collected for this study.

extending to 177 m. P-waves were generated with a sledgehammer striking a metal plate. At sites SOP and SOW, we also used a vacuum-assisted vertical weight-drop seismic source for P-wave data. The S-wave seismic source consisted of a wooden timber placed on the pavement or dirt beneath the wheels of the vehicle at right angles to the direction of the profile. Striking opposite ends of the timber with a 4-kg sledgehammer produced reversed-polarity S-waves.

2.2. Data processing

Except for site SOW, we developed the final interpretations of the data without consulting the downhole data. For site SOW, which was also the first site of investigation, we first blindly determined a preliminary V_s model that turned out to be close to the downhole result in the upper 17 m where the reflection/refraction data differed from the borehole data by an average of 13%. From 17 to 30 m depth the difference jumped to an average of 24%. The greater uncertainty in the deeper portion of the data led us to reexamine the reflection/refraction data. We had been uncertain about whether to interpret a low-amplitude group of refracted first arrivals between the second and third layers as an additional layer. Incorporating this additional layer kept the upper part of the reflection/refraction V_s model relatively unchanged and reduced the average difference between the reflection/refraction and borehole data in the 23- to 30-m depth range to about 5%. Consulting the borehole data at site SOW prior to making the final interpretation gave us the confidence to include this additional layer and to make somewhat bolder interpretations on all the other data.

We interpreted the refraction data using the slope-intercept method as described by Mooney (1984), while seismic reflections were interpreted separately using a hyperbolic curve-fitting utility within the

Table 2
Site names, locations, surficial geology, setting, and inter-site distances

Site name	Site location	Surficial geology	Cultural setting	Inter-site distance (m)	Borehole data source
FOS	Beach Park Blvd., Foster City, CA	Q estuarine	residential	100	Gibbs et al., 1994
HOL	Hollister Airport, Hollister, CA	Qal	rural airport	175	Gibbs and Fumal, 1994
KIN	Kingdome, Seattle, WA	artificial fill	City, urban	100	Perkins, 1994
PAV	Palo Alto V.A. Hospital, Palo Alto, CA	Pleistocene alluvium	urban	50	Gibbs et al., 1992
SOP	Sherman Oaks Park, Sherman Oaks, CA	Qal	residential park	0	Gibbs et al., 1996
SOW	Woodman Ave., Sherman Oaks, CA	Qal	urban	5	Gibbs et al., 1996

New interpretations of V_p and V_s downhole data at sites SOP, SOW, and FOS (V_s only) were provided by D. Boore (written communication, 1999).

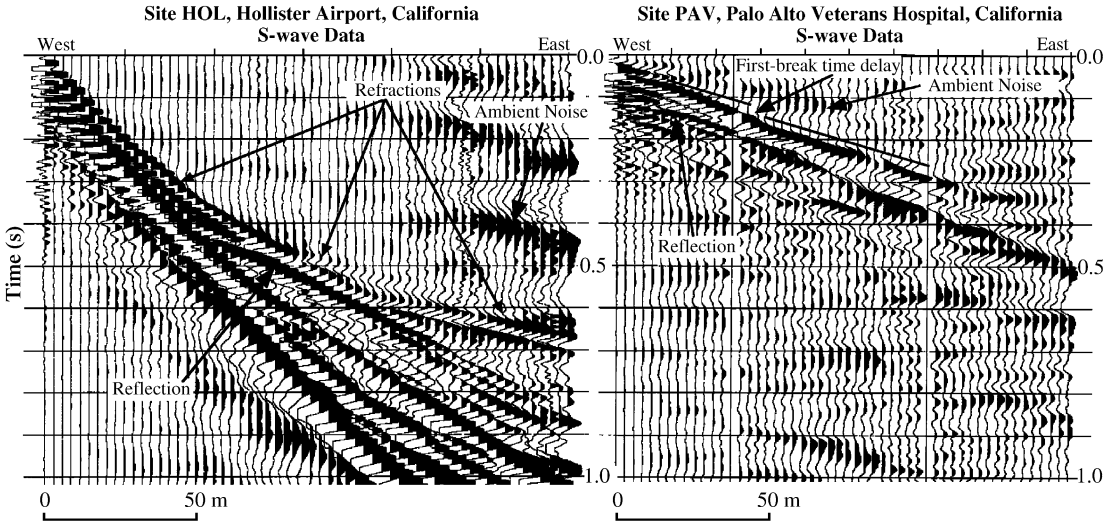

Fig. 2. S-wave seismic reflection/refraction profiles from Hollister Airport (left) and Palo Alto Veterans Hospital (right) showing the variation in ambient cultural noise. The sledgehammer impact point is at the west end of both profiles. Ambient noise is much greater over the entire record at PAV. The data from both sites displayed here were filtered with a 4.5–60 Hz bandpass. No other data processing was applied.

computer program ProMAX® (Landmark Graphics, 1998). Most commercially available engineering seismic data processing software contains a similar reflection curve-fitting tool. For the refraction data, we selected first-arrival phases, assumed to be refracted from the same interface, from an interactive video-screen display of the shot record. Velocity and the zero-offset time were then calculated from the slope of the line we fit to these phases (Fig. 3). The zero-offset times and velocities were input to a computer program (Mooney, 1984) to generate a depth section. Where the refraction first breaks were not obscured by cultural noise or attenuation, we determined that by intentionally mispositioning the line fit from the preferred slope a tolerable amount, that a maximum possible velocity variation is about 5%. On poorer quality data, the slopes are accurate to within about 10%, and because layer thickness is proportional to the product of layer velocities (e.g., Dobrin, 1976, p. 297), the accuracy of layer thickness calculations

Table 3
Generalized seismic data recording parameters

Recording system: Geometrics StrataView (30 channels)
Sampling interval: 0.001 s
Record length: 1 s
Recording format: SEG-2
Geophones: 30 vertical, 8 Hz, and 30 horizontal, 4.5 Hz
Geophone array: linear with single phones at 3-m intervals
Source: 4.0 kg sledgehammer on metal plate, or 100 kg vacuum-assisted weight drop (P-wave); 4.0 kg sledgehammer on wood timber (S-wave)
Source array: Reversed spreads, multiple off-end shots

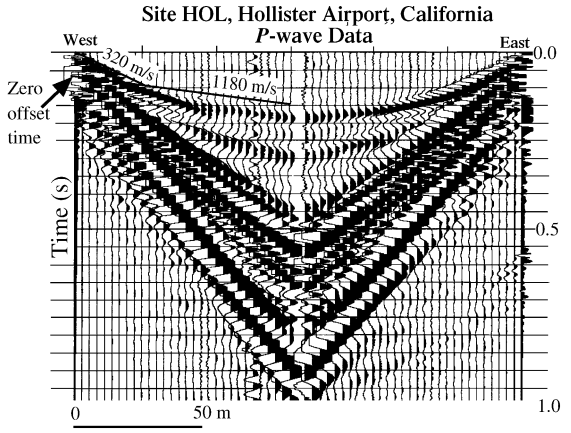

Fig. 3. Reversed P-wave seismic reflection/refraction profile from Hollister Airport showing an example of straight-line fits to the first-arrival refraction phases. The slopes of these lines give the velocity as annotated above the line. The zero-offset time is also shown for the higher velocity phase. The data are displayed without further enhancement.

decreases to about 10% to 20%. During the analysis of refraction phases, we also visually checked the data for clear reflections. If reflections were present we determined their moveout velocities and picked the zero-offset travel times to obtain depth measurements that might aid the refraction interpretation.

The P- and S-wave profile lengths resulted in a maximum survey depth range of about 30 to 50 m. At site HOL, S-wave refraction data extended the imaging depth to 80 m. In cases where no layers were detected below about 20 m by reflection or refraction methods, such as at sites PAV, FOS (P-wave data only) and KIN, we used a rule-of-thumb constraint to extend the maximum refractor imaging depth to about 30 m. This rule assumes that if the velocity increases with depth then maximum refractor imaging depth is equal to about 1/3 the length of geophone array deployed on the ground surface (Mooney, 1984). If low-velocity zones are present, then this rule-of-thumb would tend to overestimate the maximum imaging depth. The maximum geophone array lengths at PAV, FOS, and KIN were 157, 177, and 87 m, respectively, and were 177 m at all other sites.

2.3. Identifying velocity inversions in reflection/refraction data

One of the disadvantages in using reflection/refraction methods is that a velocity inversion, defined by a high-velocity layer underlain by a lower-velocity layer, can be impossible to detect by refraction methods alone or even in combination with reflection data. As will be shown in the next section some velocity inversions interpreted in the downhole data were not detected by reflection/refraction data possibly because the velocity inversions were not laterally extensive enough, or were too thin to be resolved. As a result, the reflection/refraction velocity profiles in some cases were more like an average velocity profile when compared to the downhole data. We used two interpretation techniques to identify inversions and measure their thicknesses. In technique 1, we use travel time skips or terminations in the refracted-phase arrivals to identify inversions, and in technique 2 we incorporate information from reflected phases because velocity data from these phases are an average of all overlying materials, including the low-velocity layers. Because seismic-reflection data are not adversely affected by velocity inversions, it becomes very important to also have acquired the best possible seismic reflection data. In our procedures, there is no additional time or equipment needed to acquire the reflection data because hammer impacts generate both the reflection and refraction phases recorded in our array. Curiously, in our experience, about half of the sites that contain a velocity inversion tend to also be characterized by good-quality reflection data that can compensate for the lack of refracted waves. Technique 1 is based on the results of Tewari et al. (1995) who showed that if the low-velocity layer is much thicker than the overlying higher-velocity layer, the effects of velocity inversions can sometimes be observed directly in the seismic refraction data in the form of travel time skips or delays of the first-arrival phases. Though Tewari et al. (1995) described these effects for deep crustal refraction surveys, we believe we observe these same effects in the S-wave data at sites FOS and KIN in the upper 30 m (Fig. 4).

At site FOS, we observed the fade-out and eventual termination of a first-arrival refraction phase at about 60-m offset from the source location at the north end of this shot record (Fig. 4). To estimate the thickness of this surficial layer we used a rule-of-thumb developed by Whiteley and Greenhalgh (1979) who found that in nearly all cases the cut-off distance (i.e., the distance beyond which the refraction ceased to be observed) is less than 20 to 30 times the thickness of, in this case, the surficial layer. Our surficial layer thickness estimate of 2.5 m is supported by the downhole survey (Fig. 5). A first-arrival refraction is detected again at about 70 m offset after a time delay of about 0.5 s. Because of this first-arrival pattern, we suspected that there was a velocity inversion at this site and we resorted to interpretation technique 2 that combines the limited refraction data and the good-quality reflection data recorded here to recover the velocity and depth model (Fig. 4). The reflection gives the interpreter information about the depth of the reflector and the average velocity of the overlying deposits. Since there were no other useful refraction phases from layers beneath the surficial layer we interpreted this site only through reflection analysis.

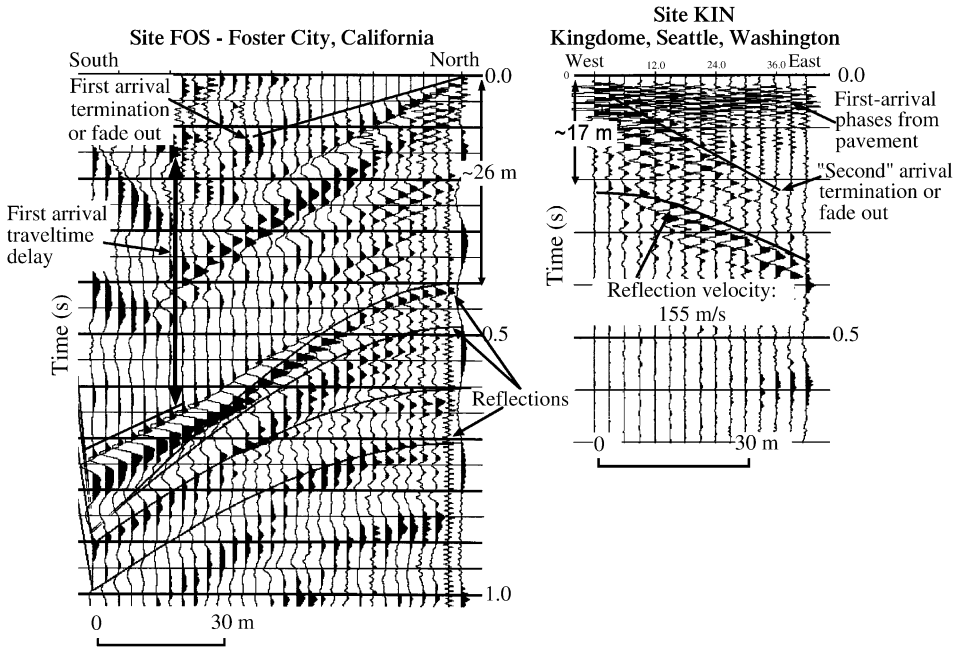

Fig. 4. S-wave seismic reflection/refraction profiles from near the Kingdome (right) and Foster City (left) showing the effects of velocity inversions on the refracted phases. At Foster City, the refracted first arrival appears to die off and then re-emerge after a time delay. At the Kingdome, the refracted arrival appears to die off. Seismic source offsets were limited at the Kingdome by high-amplitude ambient noise, so we were not able to clearly see if the first arrival picked up again after a time delay. At both locations, reflections help to compensate for the degraded refraction data. The data from site FOS displayed here were filtered with a 6–80 Hz bandpass and a 400 ms AGC scaling window length. The data from site KIN displayed here are raw data—no filters or trace amplitude scaling.

We interpreted reflection times and velocity fits of seven unique reflection hyperbolas at this site (not all shown in Fig. 4), and then used the Dix equation, described in Dobrin (1976), to determine reflector depths and the resultant V_s profile:

$$V_{\mathrm{il2}}^2 = \frac{V_2^2 T_2 - V_1^2 T_1}{T^2 - T_1},$$

where $V_{\mathrm{i}12}$ is the interval velocity between reflections 1 and 2 and V_1, V_2 are the velocities of adjacent reflections with velocities determined from the hyperbolic curve-fitting tool and T_1, T_2 are the respective zero-offset two-way travel times of the reflections.

As another example of V_s inversion effects on refracted phases, we observed at site KIN that the desired signal, probably the direct arrival from the man-made fill, is obscured by higher-velocity, rapidly attenuating high-frequency phases propagating through the pavement (Fig. 4). The V_s profile at site KIN was constructed from two seismic refraction/reflection profiles that are roughly equidistant from the borehole, one profile on the north side of the former site of the Kingdome and one profile on the southeast side. Poor data quality and a limited geophone array length of 87 m at these sites limited our interpretation. Operations at night, when ambient cultural noise is lower in this industrial area, would probably be advised for this site and other similar sites. But, as at site FOS, a high-amplitude reflection from the base of the low-velocity zone (about 17-m deep) proved to be the most reliable data to estimate the V_s in the upper 17 m (Fig. 4). For the 17 to 30 m depth interval, we interpreted a weak refraction phase at the southeast site with a 400 m/s V_s (data not shown). Comparison with the borehole at site KIN shows that our estimated V_s from 0 to 17 m is higher, and our 17 to 30 m estimate is lower than the borehole data (Fig. 5). These discrepancies in V_s may be due to subsurface differences over the 100 m distance

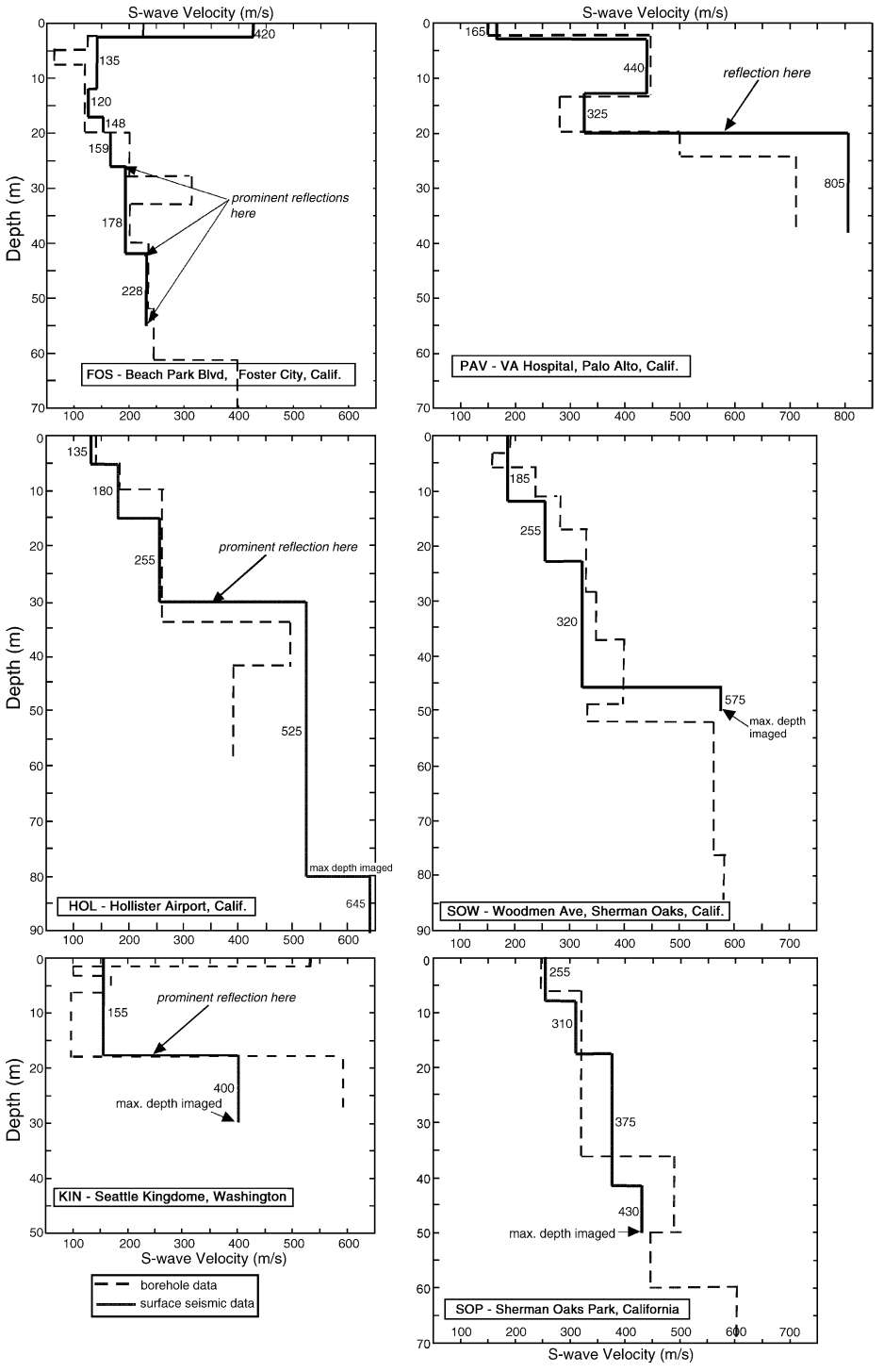

Fig. 5. S-wave velocity profiles at six locations obtained from seismic reflection/refraction data (solid line) and downhole data (dashed line).

separating the borehole site from the reflection/refraction sites, an oversimplification of our reflection/refraction data interpretation in the upper 17 m, or a combination of both. Though reflection data are not required to get P- and S-wave velocity measurements, these examples show that, in some cases, where refraction phases are weak or absent, reflection phases may be the only data available left to interpret.

3. Results

In the overall comparison of reflection/refraction and downhole data, we assessed under what conditions reflection/refraction methods can be used as opposed to downhole methods. To determine these conditions we compared the P- and S-wave data from downhole and reflection/refraction methods in three ways: (1) by visual inspection of velocity plotted as a function of depth, (2) by a comparison of average velocities to 30-m depth (V_{s30}) and the resulting NEHRP site category (S-wave data only), and (3) by a method introduced by Boore and Brown (1998) that quantifies differences between the velocity profiles using the ratio of the relative linear site amplification produced by the two profiles over a specified set of quarter-wavelength frequencies. In method 3, the quarter-wavelength amplification approximation for each velocity profile is given by the square root of the seismic impedance for ground motion averaged from the surface to a depth specified by the quarter wavelength divided by the impedance at the surface of a halfspace with density and velocity values equal to those assumed to exist at, for example, the earthquake source depth (reference depth). Visually comparing records as in method 1 above is an important qualitative component of the comparison, but it can be subjective. Thus, the third comparison technique is critical because it produces a quantitative assessment of the differences in velocity by relating these differences to the potential site amplification that could be produced by the velocity profiles. The site amplification ratio method emphasizes differences in low velocity layers near the surface that have a greater effect on travel time and might go unnoticed with a standard visual inspection by itself.

3.1. Visual comparison of downhole and reflection/refraction data velocity profiles

Using the first of the three methods of comparison, visual inspection, at four of the six sites we find general agreement (within 20%), but not duplication between the borehole data and the reflection/refraction data in S-wave velocity-versus-depth (Fig. 5). General agreement occurs in the trends of lower to higher velocity with increasing depth at all sites. Focusing on the upper 30 m, the best agreement occurs at sites HOL, PAV, SOW, and SOP, where at least 70% of the reflection/refraction V_s data in this interval is within 20% of the borehole data velocities. However, velocity agreement within 20% in the upper 30 m occurs for only 47% of the FOS reflection/refraction velocity profile and only 10% of the KIN profile. The large disagreement at site KIN is misleading because it suggests that the reflection/refraction profile has little value in characterizing the velocity structure. However, we believe it still has value for the earthquake seismologist needing a quick site characterization because the reflection/refraction profile does accurately capture the thickness of the surficial low-velocity layer indicating at least a factor of 2.5 velocity increase at the base of the low-velocity layer. Specific discrepancies between reflection/refraction and borehole data occur at sites FOS, HOL, and KIN where three significant velocity inversions (5 to 10 m thick) interpreted in the downhole data were not observed in the reflection/refraction data. Other than inadequate interpretation methods, we have no explanation as to why these inversions were not detected by seismic reflections because vertical resolution limits at these sites, about 1 to 3 m, were within the range needed for detection. Other velocity inversions were detected, for example, at site PAV a prominent velocity inversion in the borehole data was also interpreted in the reflection/refraction data by a combination of an S-wave reflection and a small time delay in the first-arrival refracted phase (Fig. 2). Systematic differences, such as the reflection/refraction velocities being consistently low or high over specific intervals, are not strongly apparent. A comparison of the relative travel time versus depth for the reflection/refraction and borehole data shown in Fig. 5 highlights the largest discrepancies at sites FOS and KIN. At site FOS, a very low borehole velocity in the 5 to 7 m depth

interval (49 m/s) causes the greatest travel time differences over the entire 59-m interval of comparison. As indicated at sites HOL, SOW, and SOP (Fig. 5), there may be a slight tendency for the reflection/refraction data velocities to be lower than the downhole data in the 0 to 20 m depth range.

3.2. Velocity profile differences at selected sites

Several factors made the reflection/refraction S-wave data at site FOS the most difficult site to interpret: velocity inversions, a lack of clear refraction arrivals, and the uncertainty in identifying reflections earlier than 400 ms (Fig. 4). A factor affecting the V_{s30}, and the biggest difference in S-wave data at site FOS, is the V_s discrepancy in the upper 2.5–3.0 m (Fig. 5). Recently, D. Boore of the U.S. Geological Survey (pers. commun., 1999) reported that this site was remeasured using downhole methods and a finer depth sampling interval than used in Gibbs et al. (1994). These new measurements increase the V_s from about 100 m/s to about 230 m/s in the upper 2.5 m and decrease the V_s to about 50 m/s from 5 to 7.5 m (Fig. 5) (D. Boore written commun., 1999). But despite these new measurements, the V_{s30} at FOS determined from Gibbs et al. (1994), remains unchanged from 125 m/s. After incorporating the new borehole data at FOS, there is still a factor of two difference in V_s between the reflection/refraction data and the downhole data in the upper 3 m. This difference could be due to differences in the near-surface deposits between the two sites. If the seismic velocity from the reflection/refraction data were the same as the borehole data in this 3.0-m interval, then the V_{s30} of the reflection/refraction data would reduce to 148 m/s; a 16% difference from the borehole data. However, we believe the reflection/refraction data are correct at site FOS because the velocity was picked from a set of about 10 stations that recorded this first arrival. Though we do not have any evidence other than the velocity measurements, the high velocity surface layer at this site may represent firmly compacted man-made fill that was originally brought in to establish Foster City. Another prominent inconsistency is the presence of an S-wave velocity inversion at about 27-m depth in the downhole data that was not detected in the reflection/refraction data. But, as shown in Fig. 5, at site FOS there are also some strong similarities in the two velocity profiles. For example, prominent S-wave reflections from depths of 26 and 55 m generally correlate with significant lithologic boundaries noted in the borehole geologic log of Gibbs et al. (1994) at depths of 25 and 62 m. Also, at site FOS, a prominent S-wave reflection from 42-m depth correlates with a soft clay/stiff clay boundary at 43 m in the geologic log. Despite the complications introduced by the velocity inversion at this site, we achieved a similar measure of the velocity structure as determined by visual inspection of the two velocity profiles in Fig. 5.

Strong ambient noise and a velocity inversion at site PAV complicated the reflection/refraction P- and S-wave data interpretation (Figs. 2 and 5). The primary difference between the two methods' interpretations of the S-wave data is that two layers were interpreted in the borehole data below about 20-m depth that were not observed in the refraction/reflection data (Fig. 5). Inspecting the reflection/refraction data, and with knowledge of the borehole data at this depth interval, we still do not observe the thin layer with a velocity of about 510 m/s at 19- to 24-m depth interpreted in the borehole data. The resolution limits of the reflection/refraction data in this depth range should be sufficient to detect a layer of this thickness. It is possible the layer is much thinner or nonexistent at the location of the reflection/refraction profile which is located about 50 m from the borehole. Nevertheless, the similar V_{s30} value for this site shown in Table 4 indicates that the reflection/refraction method gives a reliable result without knowledge of the borehole data. For the P-wave data, a higher velocity in the 13- to 20-m depth range, and a velocity inversion at about 20-m depth were interpreted for the borehole data (Fig. 6). There does appear to be evidence for both a velocity inversion, in the form of a refracted-phase termination, and a layer velocity closer to the borehole data at this depth interval. But this was not recognized initially because of ambient noise obscuring the signal. We believe that higher energy P- and S-wave seismic sources would have been helpful at this site to increase the signal-to-noise ratio.

An S-wave velocity inversion at site KIN was suspected because of the weakening and ultimately terminating arrival (Fig. 4). Consequently, the seismic velocity down to about 18-m depth from the reflection/refraction data was estimated solely from the

Table 4
Average velocities from the surface to 30-m depth and the corresponding NEHRP site classifications

Site name	Borehole V_{s30} (m/s)	Reflection/ refraction V_{s30} (m/s)	Percentage difference in V_{s30}	NEHRP site classification (borehole)	NEHRP site classification (reflection/refraction)
FOS	125	151	+21	E	E
HOL	215	196	−9	D	D
KIN	**166**	**245**	**+48**	high **E**	middle **D**
PAV	**351**	**396**	**+13**	high **D**	Low **C**
SOP	302	315	+4	D	D
SOW	258	230	−12	D	D

Interpretations resulting in sites being placed in different site categories are in shown in bold.

prominent S-wave reflection (Fig. 4). From the velocity calculated by a hyperbolic fit to this reflection, we can assume that it indicates an average velocity from the surface to the depth of the reflector. The difference in average velocity between the downhole and reflection/refraction data may be related to their slightly different locations—they are separated by about 100 m. For site characterization and earthquake site resonance reasons, its important to note that, although the V_{s30} values differ by 48%, the important impedance boundary at about 18-m depth was observed by both methods: as a high velocity contrast in the downhole data and as a prominent S-wave reflection in the reflection/refraction data. The reflection travel time at this site correlates with a potentially damaging 2-Hz resonance that was observed in earthquake seismograms from a location about 200 m west of the reflection/refraction data site (Williams et al., 1997, 1999). Another more recent example of this connection between reflection travel time and earthquake site resonance comes from the 2001 M6.8 Nisqually earthquake. On the west side of Boeing Field in Seattle, WA, we acquired an S-wave seismic reflection/refraction profile containing a prominent reflection at about 0.52 s zero-offset travel time (about 60 m depth) (Fig. 7). This travel time translates to a frequency of about 0.95 Hz using:

$$f_r = \frac{1}{2T},$$

where T is the two-way travel time of the reflection. The frequency spectrum of a seismogram recorded at this site during the Nisqually earthquake shows a high amplitude resonance at about 0.85 Hz (Fig. 7), which appears to correspond to the impedance boundary indicated by the reflection. The apparent 0.1 Hz discrepancy between the resonance calculated from the reflection time and the observed resonance could be caused by non-linear ground motions in this vicinity. Evidence of non-linear ground shaking was observed at Boeing Field during this earthquake as sand boils and ground settlements (Troost et al., 2001).

3.3. Comparing V_{s30} estimations

Systematic differences in layer velocity determinations between reflection/refraction and borehole data methods might also show up in a comparison of V_{s30}. In comparing V_{s30} we find that four of the reflection/refraction values are higher than the borehole data by varying amounts from 4% to 48% (Table 4). In terms of absolute value of V_{s30}, the best agreement (<15% difference) occurs at sites HOL, PAV, SOP, and SOW, while sites FOS and KIN differ by 21% and 48%, respectively (Table 4). Notably, the sites with velocity inversions also tend to have the largest discrepancy in average velocity values between the two methods. Unfortunately, and perhaps revealing a weakness of the NEHRP site classification system, the V_{s30} values can differ by significant amounts and still be classified in the same NEHRP site category (e.g., site FOS). Conversely, if the V_{s30} falls near a NEHRP site category boundary, such as site PAV, which is close to the 360 m/s boundary between category C and D, differences in V_{s30} can be quite small but still place them in different site categories. With these considerations, we still found that four of the six sites were in the same NEHRP site category as determined independently by reflection/refraction and downhole methods (Table 4). Given the small sam-

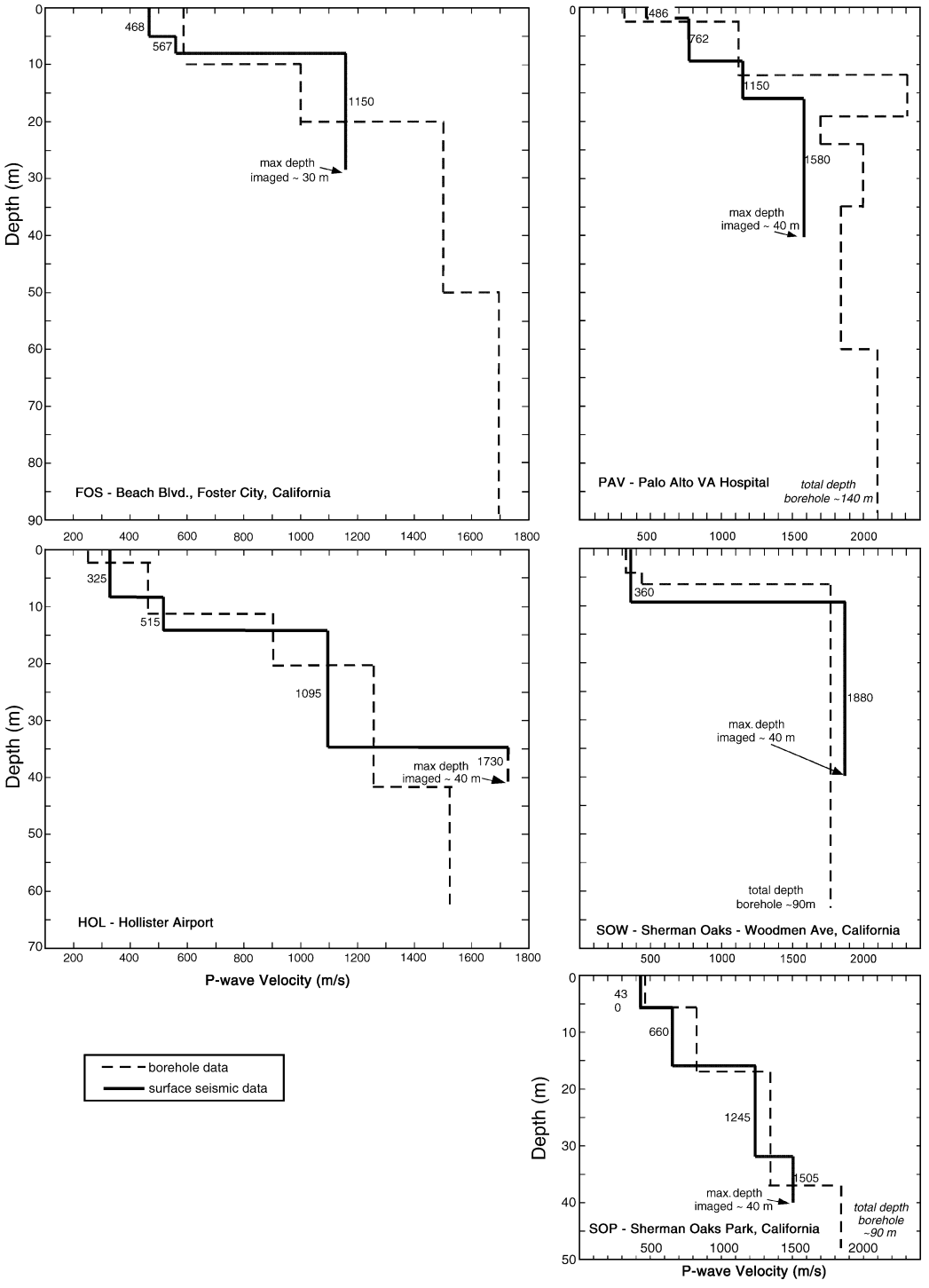

Fig. 6. P-wave velocity profiles at five locations obtained from seismic reflection/refraction data (solid line) and downhole data (dashed line).

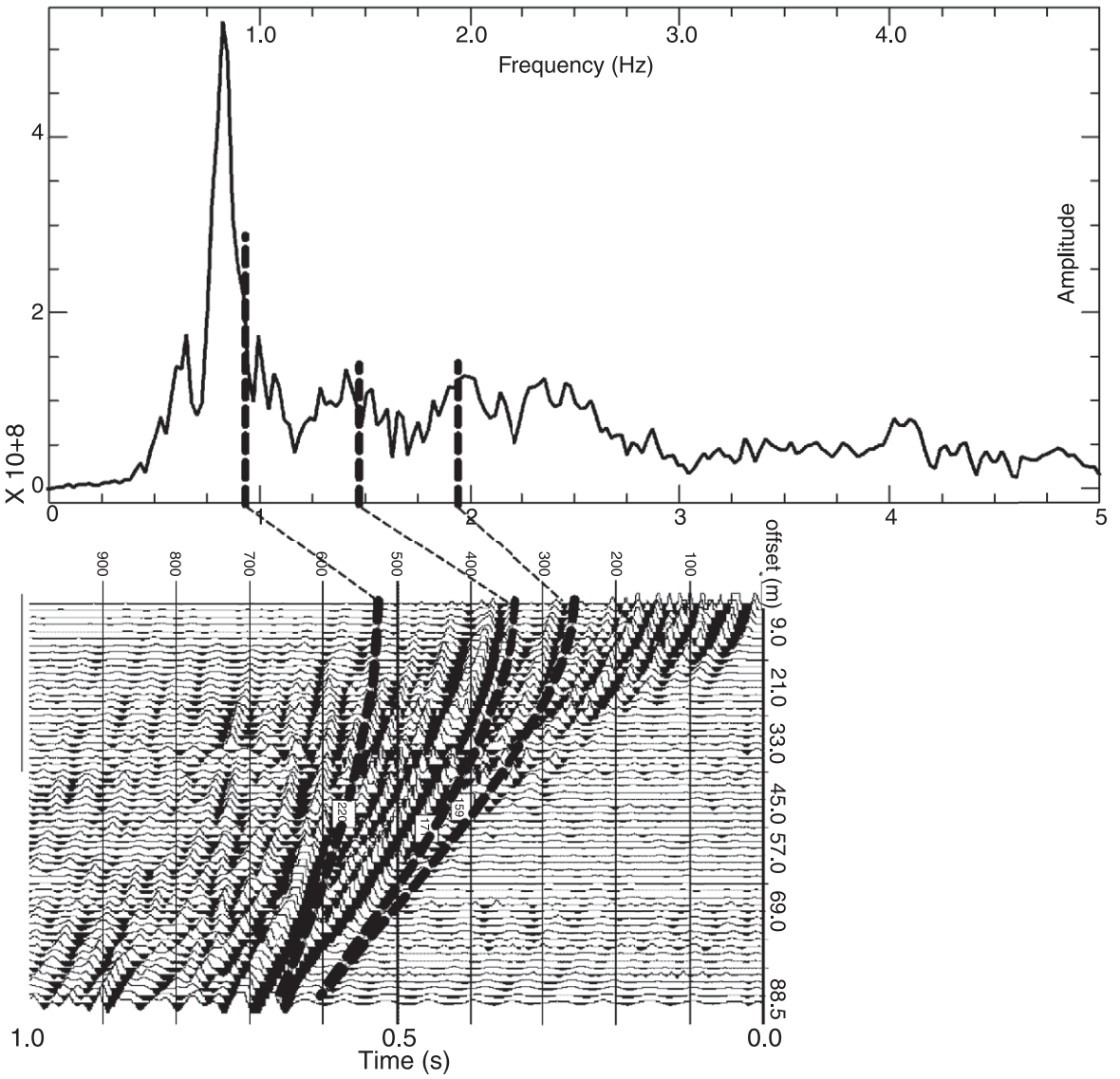

Fig. 7. Frequency spectrum of the average of the two horizontal components that recorded the M6.8 Nisqually earthquake at Boeing Field in Seattle, WA (top). S-wave seismic reflection profile recorded at this site. Dashed lines trace reflections and indicate resonance frequencies (dashed vertical lines in upper figure) predicted by zero-offset reflection times.

ple of this study, systematic differences described above may not be significant.

A recent observation we have made may simplify determinations of V_{s30} even more (Williams et al., 2001). Given the old refraction spread length rule-of-thumb described earlier, in which the maximum imaging depth is equal to about 1/3 the spread length, it occurred to us that there should be a relationship between V_{s30} and the S-wave first-arrival travel time measured on the ground surface at about 100 m from the source. To test this possibility, we examined more data than the six sites emphasized in this study. After comparing V_{s30} and travel times at the 50 and 100 m offsets points from least 36 locations in Seattle, WA, and San Jose, CA, we find the best r-squared value, 0.96 versus 0.94, is associated with the 100 m offset

travel time (Fig. 8). The empirically derived equation that describes this relationship could potentially be used to estimate V_{s30}:

$$\log(V_{s30}) = -0.938 \log(TT_{100m}) + 11.165,$$

where TT_{100m} equals the S-wave travel time at 100 m offset from the source. Another way of comparing these data is to convert the 100 m travel times to an apparent velocity (Fig. 9). The data in Fig. 9 show that in most cases the apparent velocity at 100 m is a good estimate of the V_{s30}. For example, at 32 of the 36 sites, the standard deviation is 22 m/s for the absolute value of the difference between the apparent velocity and V_{s30}. Including the other four stations lowers the standard deviation to 54 m/s. Three of these four sites with the largest difference (Fig. 9, left), all overestimate the measured V_{s30}. These sites were from the same general vicinity in Seattle, WA, and were found to have unique velocity structure; an indurated layer (probably glacial till) with a V_s of about 900 to 1000 m/s, was found at each of these sites in the 10- to 30-m depth range. This high-velocity layer appears to have decreased the travel times relative to most other sites shown in Fig. 9 and thereby increased the apparent velocity. Site JQU, located in a basalt quarry near Olympia, WA has the greatest difference between apparent velocity and V_{s30}, and when combined with the three other sites, suggests that high velocity deposits can skew the apparent velocity toward levels that are probably higher than the true value.

The general interpretation approach would be to set a geophone on the ground surface at 100 m distance from the S-wave seismic source and then proceed to stack several impacts. The interpreter then simply manually picks the first-arrival time at the 100-m offset station. To aid in identifying the first-arrival phase, it is helpful to record and overlay reverse polarity traces. Also, in the presence of significant

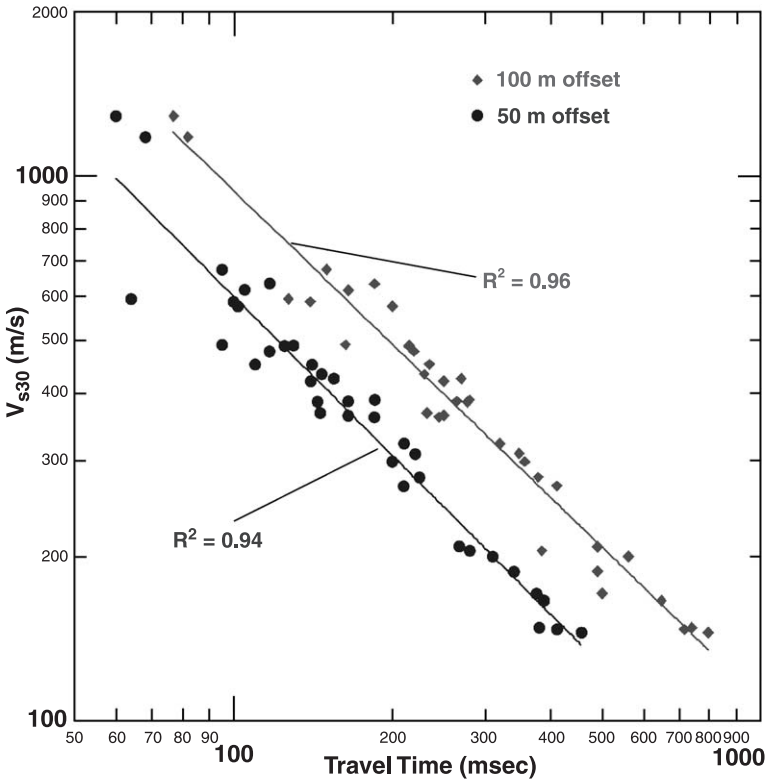

Fig. 8. First-arrival travel times measured on the ground surface at 50 (●) and 100 m (♦) distance from the seismic source plotted against the measured V_{s30} determined by reflection/refraction data.

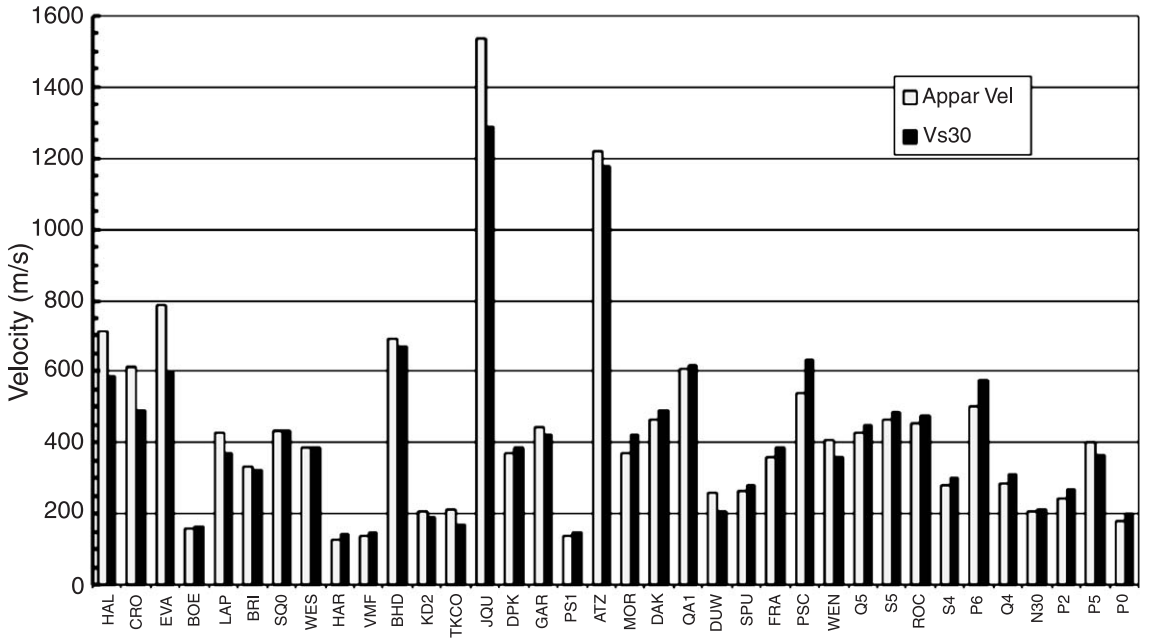

Fig. 9. A comparison of apparent velocity calculated from the 100-m offset travel time and V_{s30} determined from reflection/refraction data at 36 sites in Washington and California.

ambient noise, having several stations recorded on either side of the 100 m offset point, perhaps every 3 m, helps insure greater certainty in identifying the first arrival. To account for dipping interfaces reversed profiles are preferred but were not available for about half of the 36 sites in this dataset. Examining differences in 100 m offset travel times at the sites with reversed profiles show differences up to about 20 ms, but most appear to be within 10 ms.

3.4. Comparison of relative site amplifications

We used the method of Boore and Brown (1998) to ratio the site amplifications produced by the P- and S-wave velocity profiles of the reflection/refraction data to the downhole data. The highest frequency allowed in the comparison of S-wave data, which varies depending on the velocity profile, was determined by taking the quarter-wavelength frequency of the calculated travel time to 2.5-m depth for the reflection/refraction data. To keep the study relevant to frequencies that are important in building design, the highest frequency analyzed for the P-wave data was limited to 25 Hz. The lowest frequency in the comparison was determined by taking the quarter-wavelength frequency of the total travel time to the bottom of the reflection/refraction velocity profile. As in

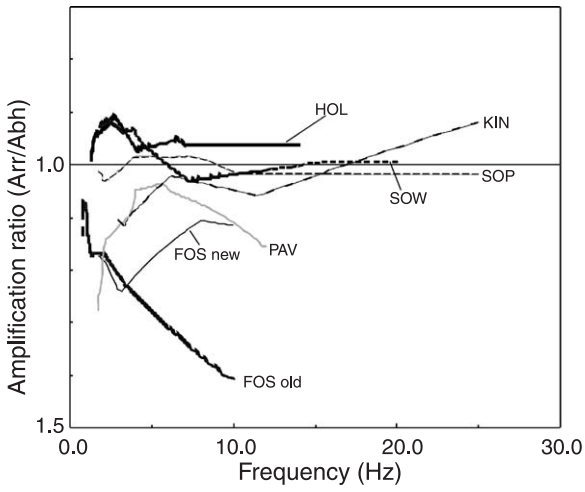

Fig. 10. S-wave site amplification ratios versus frequency for the six sites of this study. 'FOS new' and 'FOS old' refer to new downhole data (D. Boore, written commun.) and Gibbs et al. (1994), respectively.

Boore and Brown (1998), we assume that the velocity profiles converge to the same bedrock velocity at the reference depth, that the densities are the same for both models, and that the angle-of-incidence equals zero. For the purposes of this study, the variance of the amplification ratio from a value of one indicates where the velocity profiles diverge.

Because there is a relatively good match in the velocity profiles at most sites as described in earlier sections, the amplification factors of the reflection/refraction data relative to the downhole data, for both P- and S-wave velocities, tend to fall in the 0.85 to 1.1 range (Figs. 10 and 11). At no site is the amplification ratio greater than 1.4 or less than a factor of 0.7. The new downhole measurements at site FOS provided by D. Boore (written commun., 1999) significantly reduced the ratio difference (Fig. 10). The ratios from sites SOP and SOW were virtually unchanged with the new downhole measurements. It is difficult to pinpoint the exact velocity–depth intervals in each profile causing the extremes in the amplification ratios because, as noted by Boore and Brown (1998), due to velocity profile differences between the two methods, and in order to keep the compared quarter-wavelength frequencies the same, the depth interval over which the amplification ratios are formed is not exactly the same in each profile. But there are a few cases where the amplification ratio extremes can be tied to velocity mismatches between the two profiles. For example, in the reflection/refraction P-wave data at site SOW, which has a closely matched velocity–depth profile (Fig. 6), there is a bump in the ratio between 9 and 15 Hz where the reflection/refraction data amplification is up to a factor of 1.3 higher than the downhole data (Fig. 11). This bump is caused by a 1-m-thick mismatch of high velocity (1880 m/s) downhole data to low velocity (360 m/s) reflection/refraction data. Site PAV also stands out because the velocities from the reflection/refraction data are lower than those of the downhole data in the 3- to 9-m depth range (Fig. 11). In the S-wave ratios, the sites that stand out (FOS, PAV, and KIN) because the amplification factors are generally lower than the downhole data, are those with velocity inversions (Fig. 10). It appears that in the presence of a velocity inversion the velocities from the reflection/refraction data tend to be interpreted slightly higher than the downhole data.

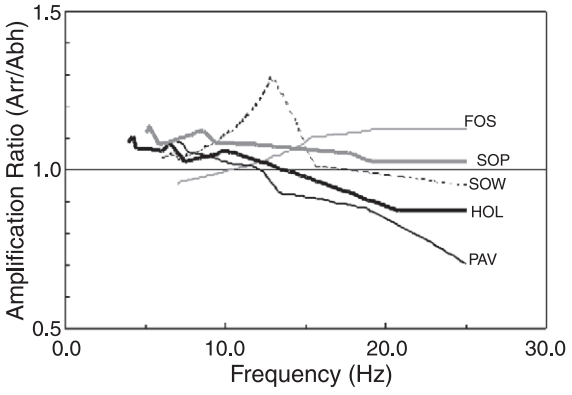

Fig. 11. P-wave site amplification ratios versus frequency for the six sites of this study. The P-wave data at site KIN were too poor to interpret and are not included.

4. Conclusions

We have established that, when compared to downhole data at six closely spaced sites located in California and Washington, surface seismic reflection/refraction data can be reliably used for measuring V_{s30} values. Surface reflection/refraction data can also give a good approximation to the more detailed downhole velocity structure, but probably cannot be substituted for it if the site characterization needs require detection, for example, of 0.5- to 1-m-thick soft clay layers in the 5- to 30-m depth range. We also found that the reflection/refraction data acquisition methods, which in some cases involved acquiring data along surface streets of busy urban areas, are fast, non-invasive, and less expensive when compared to downhole data.

Detection of some seismic velocity inversions, a major weakness of seismic refraction data, was achieved by a combination of using seismic reflection data and recognition of the effects of the inversion on the refracted-phase first breaks. However, not all velocity inversions interpreted in the downhole data were observed in the reflection/refraction data. It is clear that an exact duplication of the downhole profile cannot be achieved by reflection/refraction methods. This is probably due to differences in the properties of the deposits generated by the different subsurface area sampled by the two techniques and to the resolution limitations of reflection/refraction methods. However,

if it is not essential to exactly determine the inversion depths, that is, it is sufficient to measure an accurate estimate of the average velocity structure in the upper 30 m, then surface reflection and refraction methods are a viable cost-effective alternative.

We compared S-wave average velocities to 30-m depth (V_{s30}) for each method and found agreement within a range of 3% to 48% for an average difference of 13%. Despite the 48% difference in V_{s30} found at one site, the two methods still agreed on the depth of a critical impedance boundary at this site, which would be important for characterizing the seismic hazard. We often observe these shallow impedance boundaries as high-amplitude P- and S-wave reflections with zero-offset travel times that directly correspond to important earthquake site resonances. Converting the V_{s30} values to NEHRP site category, we determined the same category at four of the six sites. At one site, the V_{s30} value as determined by each method was only 13% different, but this difference straddled a NEHRP site category boundary and resulted in classifying the site into two different categories. Using different data from the six sites emphasized above, we also described a new approach to interpreting the surface refraction data that is solely aimed at estimating V_{s30}. In this approach, the interpreter simply notes the travel time of the first arriving phase at the geophone placed 100 m from the seismic source. The travel time at 100 m was shown to be a good estimator of V_{s30} at 32 of 36 sites.

Following a method used by Boore and Brown (1998) to compare velocity profiles by ratios of the quarter-wavelength site amplification factors, we generally found the ratios differed by 10% to 15%. Differences of up to 30% and 40% were found over limited frequency bands. The amplification calculated from reflection/refraction data at sites with velocity inversions tend to underpredict the amplification calculated from the downhole data.

Acknowledgements

We are grateful to Dr. Elizabeth Ambos (Calif. State Univ. Long Beach) and Dr. Mary Templeton (formerly of Calif. State Univ. Fullerton, now with IRIS) for providing weight-drop P-wave seismic sources at the southern California sites. We also thank Hsi-Ping Liu (USGS) for his assistance in the field, David Boore (USGS) for his use of the quarter-wavelength site amplification computer program, and James Gibbs and John Tinsley (USGS) for help in estimating costs of downhole studies and in locating some of the boreholes in the field. The manuscript was improved by reviews from John Miller, Hsi-Ping Liu, David Boore, John Ebel, James Harris, and Richard Williams. This study was supported by funding from the National Earthquake Hazards Reduction Program (NEHRP).

References

Boore, D.M., Brown, L.T., 1998. Comparing shear-wave velocity profiles from inversion of surface-wave phase velocities with downhole measurements: systematic differences between the CXW method and downhole measurements at six strong-motion sites. Seismol. Res. Lett. 69, 222–229.

Building Seismic Safety Council, 1997. NEHRP recommended provisions for seismic regulations for new buildings. Part 1—Provisions (FEMA, Federal Emergency Management Agency 302). 290 pp.

Building Seismic Safety Council, 2000. Proposals for Change to be included in the 2000 NEHRP Recommended Provisions. http://www.bssconline.org/provisions/.

Campbell, K.W., Duke, C.M., 1976. Correlations among seismic velocity, depth and geology in the Los Angeles area. Sch. Eng. Appl. Sci., 54 pp. (UCLS, UCLA-ENG-7662).

Dobrin, M.B., 1976. Introduction to Geophysical Prospecting. McGraw-Hill, New York.

Gibbs, J.F., Fumal, T.F., 1994. Seismic velocities and geologic logs from borehole measurements at seven strong-motion stations that recorded the 1989 Loma Prieta, California, earthquake, Part IV. U. S. Geol. Surv. Open-File Rep. 94-552 (89 pp.).

Gibbs, J.F., Fumal, T.E., Boore, D.M., Joyner, W.B., 1992. Seismic velocities and geologic logs from borehole measurements at seven strong-motion stations that recorded the 1989 Loma Prieta earthquake. U. S. Geol. Surv. Open-File Rep. 92-287 (139 pp.).

Gibbs, J.F., Fumal, T.F., Powers, T.J., 1994. Seismic velocities and geologic logs from borehole measurements at seven strong-motion stations that recorded the 1989 Loma Prieta, California, earthquake. U. S. Geol. Surv. Open-File Rep. 94-222 (103 pp.).

Gibbs, J.F., Tinsley, J.F., Joyner, W.B., 1996. Seismic velocities and geological conditions at twelve sites subjected to strong ground motion in the 1994 Northridge, California, earthquake. U. S. Geol. Surv. Open-File Rep. 96-740 (103 pp.).

Harris, J., Street, R., Kiefer, D., Allen, D., Wang, Z., 1994. Modeling site response in the Paducah, Kentucky, area. Earthq. Spectra 10, 519–538.

King, K.W., Carver, D.L., Williams, R.A., Worley, D.M., Cranswick, E., Meremonte, M.E., 1990. Santa Cruz seismic investi-

gations following the October 17, 1989 Loma Prieta earthquake. U. S. Geol. Surv. Open-File Rep. 90-307 (59 pp.).

Liberty, L., 1998. Seismic reflection imaging of a geothermal aquifer in an urban setting. Geophysics 63, 1285–1294.

Louie, J.L., 2001. Faster, better: shear-wave velocity to 100 meters depth from refraction microtremor arrays. Seismol. Soc. Am. Bull. 91, 347–364.

Luzietti, E.A., Kanter, L.R., Schweig, E.S., Shedlock, K.M., Van Arsdale, R.B., 1992. Shallow deformation along the Crittenden County Fault zone near the southeastern boundary of the Reelfoot Rift, northeastern Arkansas. Seismol. Res. Lett. 63, 263–275.

Miller, R.D., Anderson, N.L., Feldman, H.R., Franseen, E.K., 1995. Vertical resolution of a seismic survey in stratigraphic sequences less than 100 m deep in southeastern Kansas. Geophysics 60, 423–430.

Mooney, H.M., 1984. Handbook of Engineering Geophysics, Volume 1, Seismic. Bison Instruments, Minneapolis, MN. 103 pp.

Perkins, W.J., 1994. Kingdome seismic evaluation Seattle, Wash. Shannon and Wilson, Inc., Report W-6836-01. 210 pp.

Steeples, D.W., 1998. Shallow seismic reflection section—introduction. Geophysics 63, 1210–1212 (Special issue).

Stokoe, K.H., Nazarian, S., 1985. Use of Rayleigh waves in liquefaction studies. In: Woods, R.D. (Ed.), Proceedings of Session on Measurement and Use of Shear-Wave Velocity for Evaluating Dynamic Soil Properties. American Society of Civil Engineers, Geotechnical Engineering Division, Denver, CO, pp. 1–17.

Tewari, H.C., Dixit, M.M., Murty, P.R.K., 1995. Use of travel time skips in refraction analysis to delineate velocity inversion. Geophys. Prospect. 43, 793–804.

Troost, K.G., Booth, D.B., Shimel, S.A., Haugerud, R.A., Kramer, S.L., Kayen, R.E., Barnhardt, W.A., 2001. Geologic controls on ground failures in Seattle and vicinity during the 2001 Nisqually earthquake. Seismol. Res. Lett. 72, 353.

Whiteley, R.J., Greenhalgh, S.A., 1979. Velocity inversion and the shallow seismic refraction method. Geoexploration 17, 125–141.

Williams, R.A., Cranswick, E., King, K.W., Carver, D.L., Worley, D.M., 1994. Site-response models from high-resolution seismic reflection and refraction data recorded in Santa Cruz, California. In: Borcherdt, R.G. (Ed.), The Loma Prieta, California, Earthquake of October 17, 1989—Strong Ground Motion. U.S. Geol. Surv. Prof. Pap, vol. 1551-A, pp. A217–A242.

Williams, R.A., Stephenson, W.J., Odum, J.K., Worley, D.M., Frankel, A.D., 1997. Near-surface P- and S-wave velocities at earthquake recording stations in Seattle, Washington, from surface seismic refraction methods. EOS, Trans. Am. Geophys. Union 78, F433.

Williams, R.A., Stephenson, W.J., Odum, J.K., Meremonte, M.E., Cranswick, E., Frankel, A.D., 1998. Correlation of 1- to 10-Hz earthquake resonances with surface measurements of P- and S-wave reflections and refractions in the upper 70 m. Seismol. Res. Lett. 69, 159.

Williams, R.A., Stephenson, W.J., Frankel, A.D., Odum, J.K., 1999. Surface seismic measurements of near-surface P- and S-wave seismic velocities at earthquake recording stations in Seattle, Washington. Earthq. Spectra 15, 565–584.

Williams, R.A., Stephenson, W.J., Frankel, A.D., Odum, J.K., 2001. Using high-resolution surface seismic imaging to study earthquake site response. Geol. Soc. Am. 33, A-345 (Abstracts with Programs).